

The flux of UHECRs along the supergalactic plane using Pierre Auger Observatory data

Armando di Matteo^{a,*} for the Pierre Auger Collaboration^{b,1}

^a*Istituto Nazionale di Fisica Nucleare, Sezione di Torino,
Via Pietro Giuria 1, 10125 Turin, Italy*

^b*Observatorio Pierre Auger,
Av. San Martín Norte 304, 5613 Malargüe, Argentina*

E-mail: armando.dimatteo@to.infn.it, spokespersons@auger.org

We use the latest dataset from the surface detector array of the Pierre Auger Observatory, with events detected up to 31 December 2022 and a total exposure of $135,000 \text{ km}^2 \text{ sr yr}$, to search for possible excesses in the flux of the most energetic cosmic rays on an intermediate angular scale (top-hat radius 27° , based on our previous results) from regions along the supergalactic plane. We find no indication for any such excesses other than the previously reported one in the Centaurus region, with a post-trial significance around 3σ , which we find extends down to lower energies than previously studied. In particular, the field of view of our dataset overlaps both regions in the northern celestial hemisphere from which excesses of events have been reported by the Telescope Array. With our integral exposures over these regions comparable to the Telescope Array ones, we find no indication of any flux excesses from there, with event counts in good agreement with the expectations from an isotropic distribution.

*7th International Symposium on Ultra High Energy Cosmic Rays (UHECR2024)
17-21 November 2024
Malargüe, Mendoza, Argentina*

¹Full author list: https://www.auger.org/archive/authors_2024_11.html

*Speaker

1. Introduction

No intermediate- or small-scale anisotropies in the flux of ultra-high-energy cosmic rays (UHECRs) have been conclusively discovered yet, but a few indications for excesses above a few tens of EeV have been reported. An excess in the region around the position of the Centaurus A (Cen A) radio galaxy found in data from the Pierre Auger Observatory (Auger) [1] has reached 4.0σ post-trial significance as of the last update [2]. A correlation with the position of nearby starburst galaxies [3] has reached 3.8σ in the last update using Auger data only [2] and 4.6σ when also including data from the Telescope Array (TA) [4]. The TA “hotspot” in the Ursa Major region [5] and a new excess in the region around the position of the Perseus–Pisces Supercluster [7] have reached post-trial significances of 2.8σ and 3.3σ , respectively, as of the last update [6]. All of these regions are along the supergalactic plane (SGP), a great circle in the sky along which galaxies within $O(10^2)$ Mpc of us tend to concentrate. The Local Sheet, comprising nearly all bright galaxies within 6 Mpc of us, is also aligned with the SGP to within 8° [8]. Since at the highest energies UHECR propagation lengths are $\lesssim O(10^2)$ Mpc, a correlation with the SGP would not be surprising—though it should be kept in mind that during their propagation UHECRs can be deflected by magnetic fields by several tens of degrees. In ref. [9] we found no statistically significant excess of events in bands of 1° – 30° around the whole SGP ($p = 0.13$ post-trial); here, we will search for excesses of events in smaller regions along the SGP.

2. The dataset

In this work, we use events with energies $E \geq 20$ EeV detected by the Auger surface detector (SD) array from 2004 to 2022 inclusive, excluding the SD stations whose electronics had already undergone the AugerPrime upgrade from the events detected in 2021 and 2022. The quality cuts are optimized for high-energy medium-scale anisotropies, as in ref. [9], resulting in a total exposure of $135,000 \text{ km}^2 \text{ sr yr}$. The total systematic uncertainty on the energy scale is $\pm 14\%$, and the resolution is $\sim 7\%$ in energy and $< 1^\circ$ in arrival direction. We achieve a field of view (FoV) covering all declinations $-90^\circ \leq \delta < +44.8^\circ$ by combining vertical events (with zenith angles $\theta < 60^\circ$) with inclined ones (with $60^\circ \leq \theta < 80^\circ$). We rescale vertical and inclined exposures proportionally to numbers of events (respectively 6,896 and 1,936). As a result, the analysis is pretty robust to possible systematics affecting vertical and inclined events differently.

3. Analysis method

In this work, we use the energy thresholds $E_{\min} \in \{20 \text{ EeV}, 25 \text{ EeV}, 32 \text{ EeV}, 40 \text{ EeV}, 50 \text{ EeV}, 63 \text{ EeV}\}$, i.e. $\{10^{19.3} \text{ eV}, 10^{19.4} \text{ eV}, \dots, 10^{19.8} \text{ eV}\}$ rounded to the nearest EeV. For each such threshold, we consider all possible top-hat windows of radius $\Psi = 27^\circ$ (i.e. the radius maximizing the significance of the excess with $E_{\min} = 38$ EeV in ref. [9]) such that (1) the window intersects the SGP ($|B_{\text{center}}| \leq \Psi$) and (2) the center of the window is inside the Auger FoV ($\delta_{\text{center}} < +44.8^\circ$). For each threshold and each such window, we computed the numbers events above the threshold inside and outside the window N_{in} and N_{out} , the integrated exposures \mathcal{E}_{in} and \mathcal{E}_{out} , the expected background $N_{\text{bg}} = N_{\text{out}}\mathcal{E}_{\text{in}}/\mathcal{E}_{\text{out}}$, the estimated flux ratio $\overline{\Phi_{\text{in}}/\Phi_{\text{out}}} = N_{\text{in}}/N_{\text{bg}}$ the local Li–Ma significance Z_{LM} , and the frequentist 99% CL upper limit (U.L.) on $\Phi_{\text{in}}/\Phi_{\text{out}}$.

E_{\min}	N_{tot}	1st maximum							2nd maximum								
		L	B	$\frac{\mathcal{E}_{\text{in}}}{\mathcal{E}_{\text{tot}}}$	N_{bg}	N_{in}	$\frac{\Phi_{\text{in}}}{\Phi_{\text{out}}}$	Z_{LM}	99% U.L.	L	B	$\frac{\mathcal{E}_{\text{in}}}{\mathcal{E}_{\text{tot}}}$	N_{bg}	N_{in}	$\frac{\Phi_{\text{in}}}{\Phi_{\text{out}}}$	Z_{LM}	99% U.L.
20 EeV	8832	162°	-6°	9.56%	829.	990	$1.19^{+0.04}_{-0.04}$	+5.2 σ	1.29	241°	-5°	10.27%	900.	971	$1.08^{+0.04}_{-0.04}$	+2.2 σ	1.17
25 EeV	5380	161°	-9°	9.56%	504.	608	$1.21^{+0.05}_{-0.05}$	+4.2 σ	1.33	275°	-19°	8.00%	426.	482	$1.13^{+0.05}_{-0.05}$	+2.6 σ	1.26
32 EeV	2936	163°	-8°	9.68%	276.	363	$1.32^{+0.08}_{-0.07}$	+4.7 σ	1.50	276°	-17°	7.89%	229.	264	$1.15^{+0.08}_{-0.07}$	+2.2 σ	1.34
40 EeV	1533	162°	-6°	9.56%	140.	208	$1.49^{+0.11}_{-0.11}$	+5.1 σ	1.77	345°	-7°	1.00%	15.2	26	$1.71^{+0.36}_{-0.32}$	+2.5 σ	2.68
50 EeV	713	161°	-7°	9.56%	64.4	103	$1.60^{+0.18}_{-0.16}$	+4.2 σ	2.05	322°	-22°	3.69%	25.9	39	$1.51^{+0.26}_{-0.23}$	+2.4 σ	2.20
63 EeV	295	163°	-3°	9.56%	26.3	46	$1.75^{+0.30}_{-0.26}$	+3.3 σ	2.54	223°	+26°	9.56%	26.7	42	$1.57^{+0.28}_{-0.25}$	+2.6 σ	2.31

Table 1: Information about the excess windows shown in Figure 1, where $N_{\text{tot}} = N_{\text{in}} + N_{\text{out}}$, $\mathcal{E}_{\text{tot}} = \mathcal{E}_{\text{in}} + \mathcal{E}_{\text{out}}$, L and B are the supergalactic coordinates of the center of the window, and all other symbols are defined in section 3

	Telescope Array									Pierre Auger Observatory								
	E_{\min}	N_{tot}	$\frac{\mathcal{E}_{\text{in}}}{\mathcal{E}_{\text{tot}}}$	N_{bg}	N_{in}	$\frac{\Phi_{\text{in}}}{\Phi_{\text{out}}}$	Z_{LM}	99% L.L.	post-trial	E_{\min}	N_{tot}	$\frac{\mathcal{E}_{\text{in}}}{\mathcal{E}_{\text{tot}}}$	N_{bg}	N_{in}	$\frac{\Phi_{\text{in}}}{\Phi_{\text{out}}}$	Z_{LM}	99% U.L.	
(a)	57 EeV	216	9.47%	18.0	44	$2.44^{+0.44}_{-0.39}$	+4.8 σ	1.60	2.8 σ	44.6 EeV	1074	1.00%	10.7	9	$0.84^{+0.31}_{-0.25}$	-0.5 σ	1.76	
(b1)	$10^{19.4}$ eV	1125	5.88%	64.0	101	$1.58^{+0.17}_{-0.16}$	+4.1 σ	1.22	3.3 σ	20.5 EeV	8374	0.84%	70.1	65	$0.93^{+0.12}_{-0.11}$	-0.6 σ	1.23	
(b2)	$10^{19.5}$ eV	728	5.87%	41.1	70	$1.70^{+0.22}_{-0.20}$	+4.0 σ	1.25	3.2 σ	25.5 EeV	5156	0.84%	43.5	39	$0.90^{+0.15}_{-0.14}$	-0.7 σ	1.29	
(b3)	$10^{19.6}$ eV	441	5.84%	24.6	45	$1.83^{+0.31}_{-0.27}$	+3.6 σ	1.23	3.0 σ	31.7 EeV	2990	0.87%	26.0	27	$1.04^{+0.21}_{-0.19}$	+0.2 σ	1.61	

Table 2: Same as Table 1 for the four windows reported by TA, using the same radii and thresholds

4. Results

The local Li–Ma significance and estimated flux ratio as a function of the window center position are plotted in Figure 1. Quantitative information about the maximum-significance window for each energy threshold is reported in Table 1. We find that the most significant excess is consistently found with a window center within a few degrees of the position of Cen A regardless of the energy threshold. The strength of the excess grows with the energy threshold, but its statistical significance does not, due to decreasing statistics at the highest energies. When penalized for scanning over the energy thresholds and window positions, the 5.2 σ pre-trial significance found with $E_{\min} = 20$ EeV near Cen A corresponds to a 3.1 σ post-trial significance. No other window not overlapping with the main excess one achieves a statistical significance of more than 2.7 σ regardless of the energy threshold. As shown in Figure 2, we can set stringent upper limits to any other flux excesses, except with the highest energy thresholds and near the edge of our FoV.

In particular, the TA collaboration [6] reported excesses from certain windows in the Northern Hemisphere whose centers are inside the Auger FoV (Figure 3), but in Figure 1 no clear indications of any excesses are visible at those positions when using similar energy thresholds. To check these reports with our dataset, we repeated the analysis for those particular positions using the same window radii ($\Psi = 25^\circ$ for (a) and 20° for (b1–b3)) and energy thresholds (converted from the TA to the Auger energy scale using ref. [4, eq. (1)]) as in the TA report. The expected distributions of Auger N_{in} based on either isotropy or the TA results are shown in Figure 4, and our results in Table 2. In spite of comparable integrated exposures (similar N_{bg}) within those windows, our data do not confirm the TA reported excesses and are in good agreement with isotropic expectations. On the other hand, in each window there are possible values of $\Phi_{\text{in}}/\Phi_{\text{out}}$ that neither dataset can exclude at the 99% C.L., e.g. 1.68 in (a), 1.225 in (b1), (One caveat is that this analysis implicitly assume a flux excess uniform within the window; an excess more concentrated in the north than in the south of the window would be underestimated using Auger data, due to the strong declination

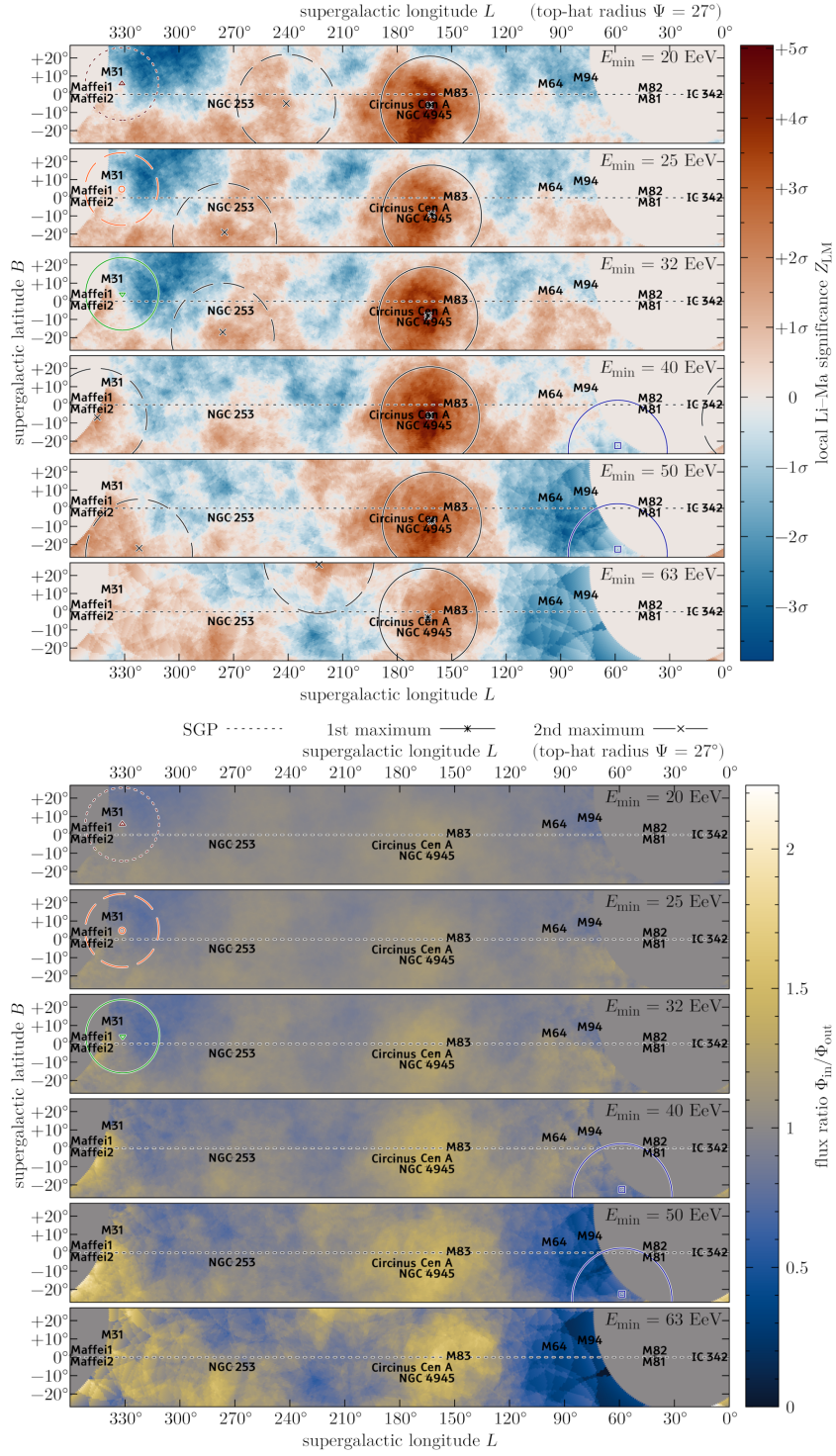


Figure 1: Local Li–Ma significance (top) and estimated flux ratio (bottom) as a function of the window center position. Each panel corresponds to the energy threshold written in its top right corner. In each panel of the top plot, the solid line is the window maximizing the local significance over the whole region we studied, and the dashed line is the most significant one among those not overlapping with the first maximum one (i.e. distance between centers greater than the sum of radii). The colored circles show the positions of the excesses reported by TA (Figure 3).

POS (UHECR2024) 006

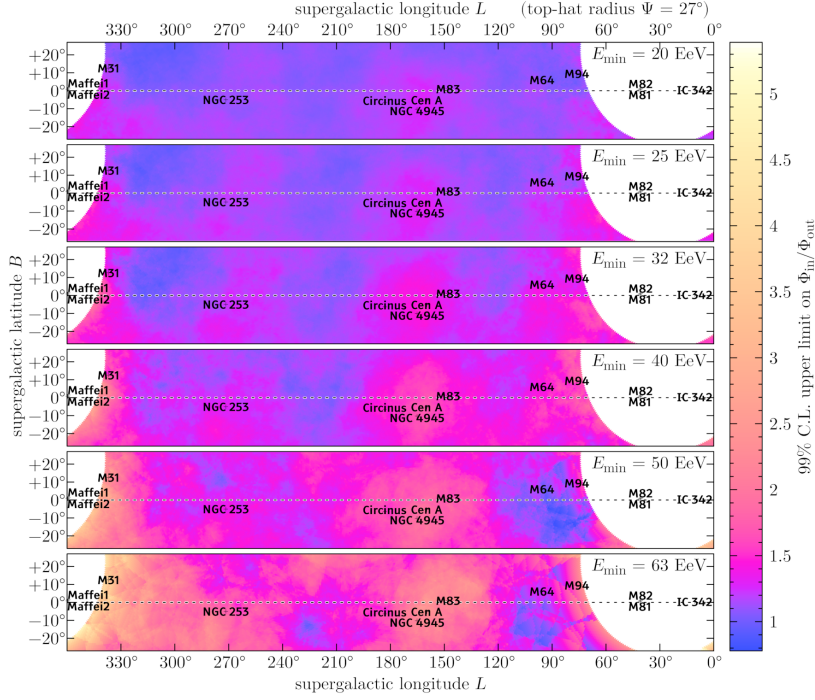


Figure 2: The frequentist 99% CL U.L. on Φ_{in}/Φ_{out} in each window reported in Figure 1

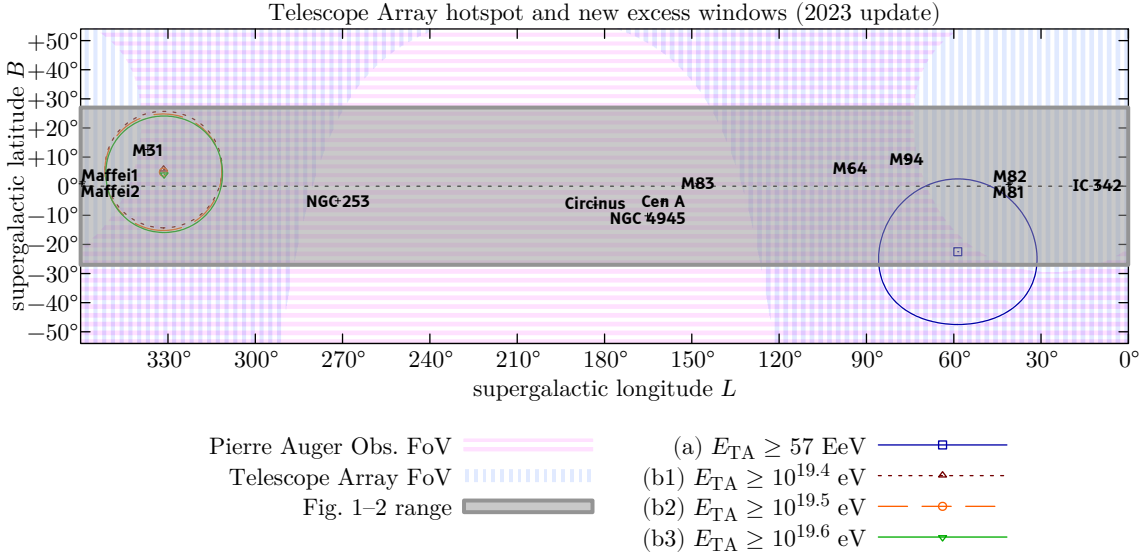


Figure 3: The circular windows from which the TA collaboration [6] reported excesses, compared with the FoVs of the two observatories and the supergalactic latitude band studied in this work. Compare with Figure 1, keeping in mind that each point of those maps corresponds to the center of a window, and that $57 \text{ EeV}_{TA} \approx 45 \text{ EeV}_{Auger}$, $10^{19.4} \text{ eV}_{TA} \approx 20 \text{ EeV}_{Auger}$, $10^{19.5} \text{ eV}_{TA} \approx 25 \text{ EeV}_{Auger}$, and $10^{19.6} \text{ eV}_{TA} \approx 32 \text{ EeV}_{Auger}$ [4].

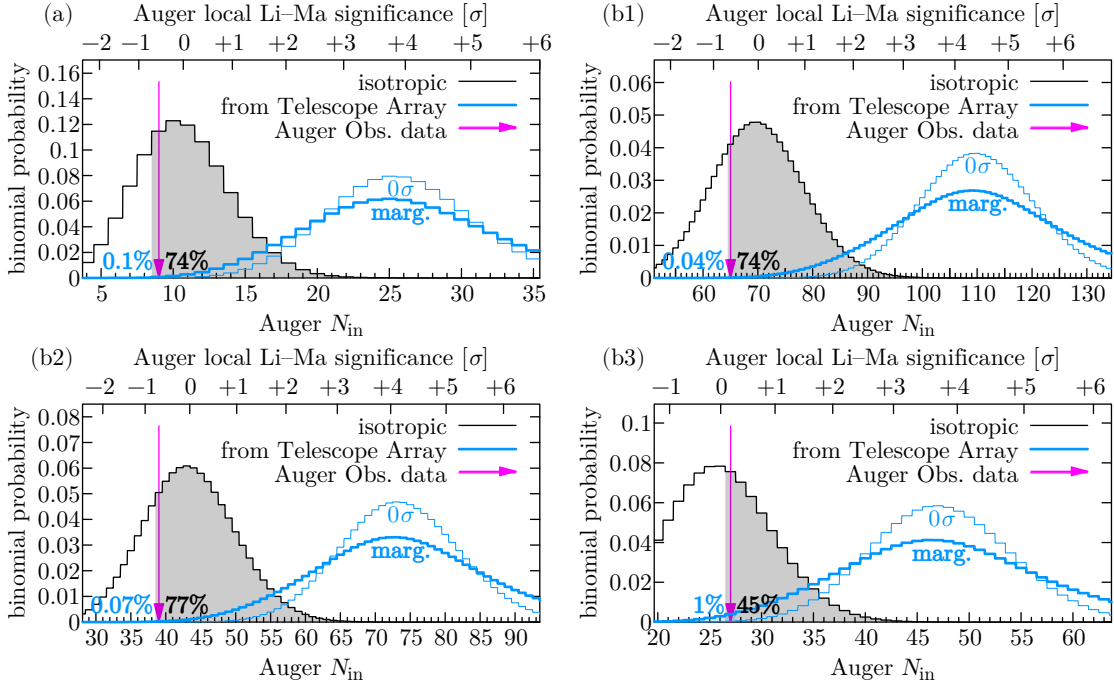


Figure 4: Distribution of the number of events expected in the Auger dataset assuming either isotropy or the TA result, compared to the actual observed number. The thin blue line assumes the central value reported by TA, whereas the thick one is a marginalization over its statistical uncertainty.

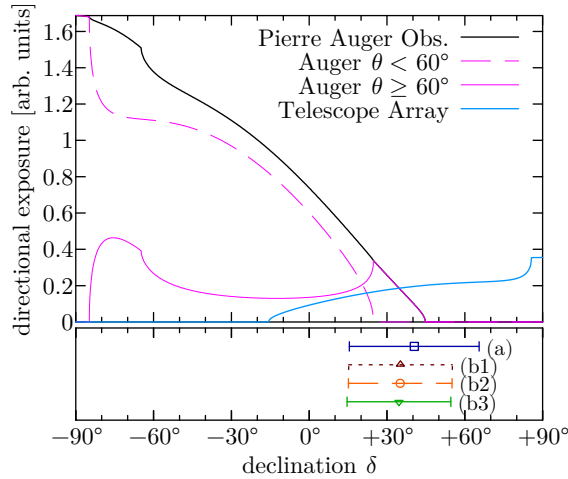


Figure 5: The directional exposure of the two observatories as a function of declination (top) compared to the declinations of the TA excess windows (bottom). The bar lengths denote the sizes of the windows, not the uncertainties in their positions.

POS (UHECR2024) 006

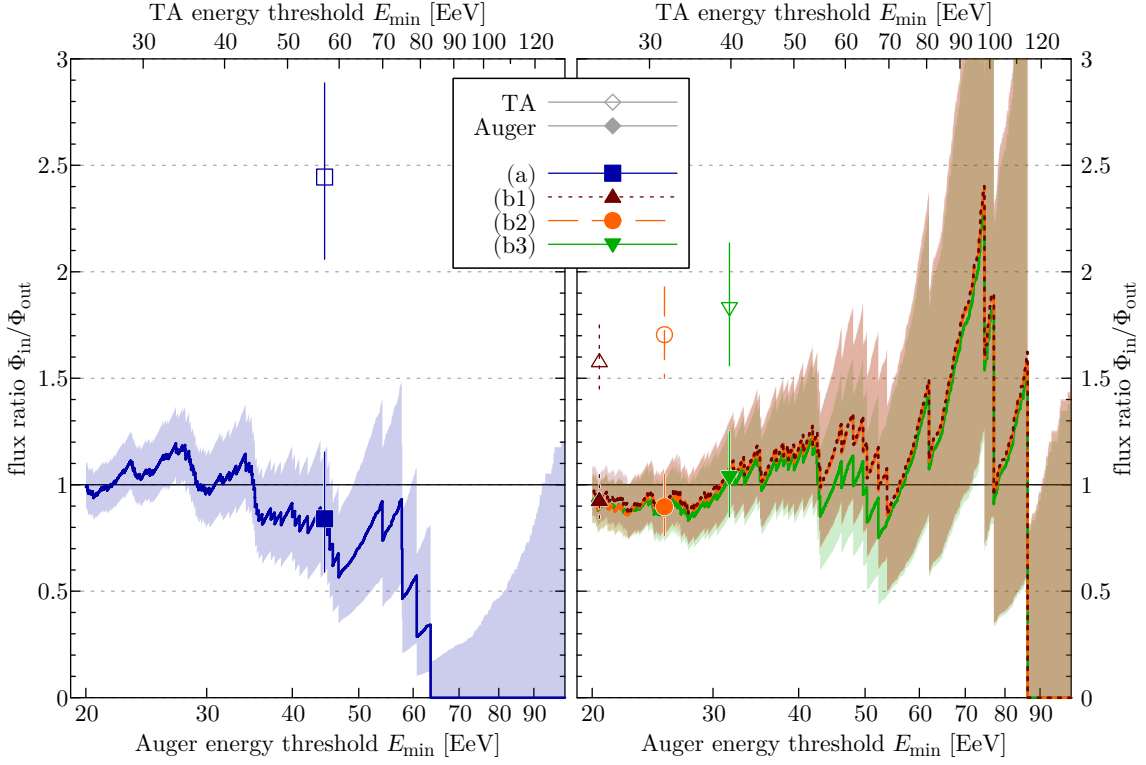


Figure 6: Flux ratio in the windows where TA reports excesses of events estimated from Auger data as a function of the energy threshold. The shaded bands are $\pm 1\sigma$ statistical uncertainties. The conversion from Auger to TA energy thresholds is based on ref. [4, eq. (1)]; the uncertainty in the conversion is comparable to the horizontal size of the markers.

dependence of the Auger exposure within these windows, shown on Figure 5. On the other hand, the declinations of the windows reported by TA were the result of a scan, so such an asymmetry would presumably have resulted in a more northern maximum-significance window position.) In order to check whether this discrepancy might be due to an inexact conversion of the threshold between the two energy scales, we repeated the analysis using a variety of thresholds (Figure 6), but found no indication for any excess from any of those windows with any other threshold either.

5. Conclusions

The previously reported indication for an excess near Cen A is tentatively confirmed with a post-trial significance of 3.1σ , extending at least down to 20 EeV in the same position of the sky, suggesting an approximately constant rigidity (i.e. atomic number proportional to the energy) of the particles making up the excess. We found no strong indication for excesses anywhere else along the SGP. In particular, our data does not confirm the indications reported by TA. More statistics would be needed to know whether any flux excesses are actually present at those positions; it will be interesting to study data from AugerPrime, TA $\times 4$, and later future observatories such as GRAND, POEMMA and GCOS once they become available. In case any excesses are confirmed, it will be interesting to study whether their mass composition differ from the background using new event-

by-event mass information such as that provided by upgraded detectors and/or machine learning techniques.

References

- [1] P. Abreu et al. [Pierre Auger Collab.], *Update on the correlation of the highest energy cosmic rays with nearby extragalactic matter*, *APh* **34** (2010) 314 [1009.1855].
- [2] G. Golup [for the Pierre Auger Collab.], *An update on the arrival direction studies made with data from the Pierre Auger Observatory*, *PoS ICRC2023* (2023) 252.
- [3] A. Aab et al. [Pierre Auger Collab.], *An Indication of anisotropy in arrival directions of ultra-high-energy cosmic rays through comparison to the flux pattern of extragalactic gamma-ray sources*, *ApJL* **853** (2018) L29 [1801.06160].
- [4] L. Caccianiga et al. [for the Pierre Auger and Telescope Array collabs.], *Update on the searches for anisotropies in UHECR arrival directions with the Pierre Auger Observatory and the Telescope Array*, *PoS ICRC2023* (2023) 521.
- [5] R.U. Abbasi et al. [Telescope Array collab.], *Indications of intermediate-scale anisotropy of cosmic rays with energy greater than 57 EeV in the northern sky measured with the Surface Detector of the Telescope Array experiment*, *ApJL* **790** (2014) L21 [1404.5890].
- [6] J. Kim et al. [for the Telescope Array collab.], *Anisotropies in the arrival direction distribution of ultra-high energy cosmic rays measured by the Telescope Array surface detector*, *PoS ICRC2023* (2023) 244.
- [7] R.U. Abbasi et al. [Telescope Array collab.], *Indications of a cosmic ray source in the Perseus-Pisces Supercluster*, [arXiv:2110.14827](https://arxiv.org/abs/2110.14827).
- [8] M.L. McCall, *A Council of Giants*, *MNRAS* **440** (2014) 405 [1403.3667].
- [9] P. Abreu et al. [Pierre Auger Collab.], *Arrival directions of cosmic rays above 32 EeV from Phase One of the Pierre Auger Observatory*, *ApJ* **935** (2022) 170 [2206.13492].